PICO-SATELLITE ORBIT CONTROL BY VACUUM ARC THRUSTERS AS ENABLING TECHNOLOGY FOR FORMATIONS OF SMALL SATELLITES

Igal Kronhaus(1), **Mathias Pietzka**(2), **Klaus Schilling**(3), **and Jochen Schein**(4)
(1)(3)Computer Science VII: Robotics and Telematics, Wuerzburg University,
Am Hubland, 97074, Wuerzburg, Germany, +49-931-31-89867,
kronhaus@informatik.uni-wuerzburg.de
(2)(4) Institute for Plasma Technology and Mathematics (EIT 1), University of the Federal Armed Forces, Werner-Heisenberg-Weg 39, 85577, Neubiberg, Germany,
+49-089-600-43765, mathias.pietzka@unibw.de

Abstract: *The possibility of maintaining pico-satellites in formation using very-low-power electric propulsion (< 2 W) is presented. The required mission propulsion performance is derived from a perturbation analysis of actual two-line elements data and high precision numerical simulation. A model predictive controller is used to develop a simple control scheme that avoids the need for on-line orbit determination. A suitable vacuum arc thruster propulsion system is presented, designed specifically for pico-satellite use.*

Keywords: *Pico-Satellite, Electric Propulsion, Orbit Control, Attitude Control, Vacuum Arc Thruster.*

1. Introduction

Considerable attention is given in the last years to the problem of lowering cost and time associated with the development of Earth observation and communication satellites, both for military and civilian uses [1],[2]. One possible method of addressing these needs is by replacing a single large spacecraft with a distributed system of small satellites [3],[4].

An active research and development effort in this field is being carried out at Wuerzburg University. A series of pico-satellites are being developed that conform to the 1U CubeSat standard [5]. The UWE (University Wuerzburg Experimental) satellite program is intended to demonstrate enabling technologies for cooperating distributed small satellites, with the eventual goal of realizing such a system in space. The UWE-4 pico-satellite is the first in the series to incorporate a propulsion system.

This paper is organized in the following way: the propulsion requirements, for a minimum pico-satellite formation mission, are discussed in section 2; the orbit control strategy is presented in section 3 and the UWE-4 propulsion system implementation is presented in section 4.

2. Mission Analysis

Due to the very limited resources available to an individual spacecraft in a pico-satellite group, only minimal demands are placed on the configuration of the formation. A practical requirement is to keep a bounded formation, where the satellites are within line of sight with each other and a ground location. Thus, relative distances of below 1500 km (about half of the maximum range) throughout the mission duration (few months) have to be sustained. It will be shown next that this requirement is not achievable without the use of thrust in low Earth orbit (LEO).

2.1. Formation Separation without Orbit Control

A group of pico-satellites can readily be deployed in a single launcher, where multiple pico-satellites are carried as a secondary payload. Typically these launches are made to circular LEO orbits. Once in orbit the pico-satellites are deployed using a mechanical separation mechanism. Thus, a relatively tight formation is formed directly after deployment. Nevertheless, without propulsion the initial formation will disperse due to orbit perturbations. Although the satellites are in nearly identical ephemeris, small variations in the semi-major-axis (SMA) and the J2 perturbation cause the satellites to drift apart. The drag is considered a secondary effect as it similarly affects all the satellites in the group.

We examine a typical case of pico-satellite formation using two line elements (TLE) data. A group of four 1U CubeSats (ITUPSAT-1, UWE-2, SWISSCUBE, BEESAT) were launched to a sun-synchronous circular orbit at an altitude of ~ 715 km. The satellites do not have a propulsion capability thus their orbit is naturally evolving. Although the CubeSats are released from the same launcher they display strong differences in drift rate as shown in Fig. 1. In the “best case scenario” after three months the relative distance between pair of satellites has increased to about 500 km. The two other satellites have drifted rapidly to thousands of kilometers.

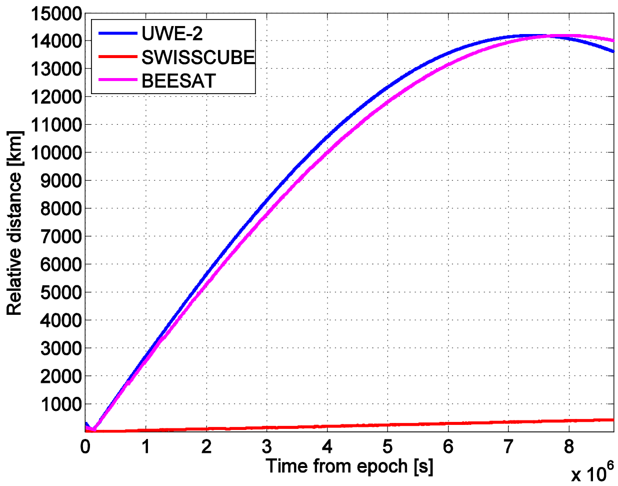

Figure 1. Relative distances between four CubeSats

2.2 Drift Rate Analysis

Considering that initially the relative distance between satellites in the group ρ is small, we expect that the differential J2 drift (as manifested in the rate of change of the right ascension of ascending node angle $\Delta\Omega$) will be less important compared to the drift caused by the Δa. The effect on the in-track secular drift rate can be approximated by the following model (see for example in [3]):

$$\dot{\rho}_{\Delta a} \sim 3/2\, n \Delta a \,, \qquad (1)$$

where $n = \sqrt{\mu / a_0^3}$ is the angular velocity of the "chief" (or reference) satellite in the group. The differential secular J2 drift effect can be evaluated by:

$$\dot{\rho}_{\Delta J2} \simeq \left| a_0 \dot{\Omega}_0 - a_i \dot{\Omega}_i \right| \approx \frac{3}{2} \sqrt{\mu} J_2 R_e^{\ 2} \left| \frac{\cos i_0}{a_0^{\ 5/2}} - \frac{\cos i_i}{a_i^{\ 5/2}} \right|, \qquad (2)$$

where $J_2 = 1.0827 \cdot 10^{-3}$ is Earth's radius, μ is the Earth's standard gravitational parameter, a_i and i_i are the SMA and inclination of each satellite respectively. By evaluating Eq. (1) and Eq. (2) together with the TLE data in Tab. 1, taken one month after deployment, we obtain that $\dot{\rho}_{\Delta J2} / \dot{\rho}_{\Delta a} \ll 1$. Thus we ignore the J2 effect and consider that the relative drift is only caused by the Δa effect.

Table 1. Orbital Parameters from TLE of Two CubeSats after 1 Month.

a_0	a_1	i_0	i_1	$\Delta\Omega$	ρ
7099.1 km	7098.8 km	98.363^0	98.358^0	0.019^0	118.3 km

The initial group formation can be determined from the first available TLE and extrapolated by the SGP4 model to the initial time of satellite deployment. However, using TLE data alone can lead to significant errors in determining the orbital parameters. TLE data are considered accurate to few kilometers, whereas the difference in SMA between satellites Δa can be smaller than few hundred meters. In order to obtain an estimate on the TLE data accuracy and determine the initial formation, the scenario is evaluated by using a drift rate match technique.

The drift rate analysis is performed by first creating a linear fit to ρ(t), where data are taken from the first few dozen TLE measurements of a satellite pair. A good linear fit is obtained as the drift rates are nearly constant in this period of time rate (in accordance to Eq. 1 but with a different constant coefficient). This averaged drift rate is compared with the drift rate calculated using a precision numerical orbit-propagator simulating a deputy satellite with an initial separation Δa. The Δa that fits the measured drift rate is considered a better estimate than the difference between TLE measurements, as it is based on multiple data points.

The results of the drift rate match analysis as well as the SGP4 extrapolation estimates are provided in Tab. 2. In one of the cases a discrepancy of 1.5 km is found between the methods. This can result in a miss-identification of a satellite in the group when using the later technique.

Table 2. Estimated Initial SMA Differences between CubeSats in the Formation

Initial SMA difference	Drift rate match	SGP4
Δa_{01} [m]	30	96
Δa_{02} [m]	1900	370
Δa_{03} [m]	2000	1890

3. Orbit Control using Very Low Power Electric Propulsion

To reduce the secular drift between satellites an energy matching principal can be employed [3]. In the case of a circular orbit of the chief, the energy principle degenerate to minimization of the Δa. Thus, in-track thrusting is selected as the control strategy for formation keeping: increasing/decreasing the deputy spacecraft SMA to match the chief's SMA, without affecting other orbital parameters. Thrust levels of few µN are assumed.

In order to analyze the relative motion between the deputy and chief, a local vertical local horizontal (LVLH) frame is selected where the origin moves with the chief satellite. The simulations are performed using a high precision numerical orbit-propagator that includes the Earth geopotential (EGM 96) and drag effects.

3.1. Phasing Maneuver

Under the assumption of complete knowledge of both chief's and deputy's orbits, a thrust control can be manually computed according to the rate of change in Δa versus the thrust applied. The applied control will then match the SMA of the deputy to that of the chief's. By performing the maneuver as close as possible to the formation deployment epoch small relative distances can be easily maintained throughout the mission.

We present an example using the worst case separation (case 3 in Tab. 2). The relative distance between the chief and deputy and the acceleration applied are shown in Fig. 2. The maneuver is performed with the deputy decelerating in the in-track direction at $a_y = 2\times10^{-6}$ m/s^2 for 5.5 days with a total $\Delta V \approx 1$ m/s. The relative stability of the new orbit is clearly shown - keeping the relative distance less than 300 km for the three months duration.

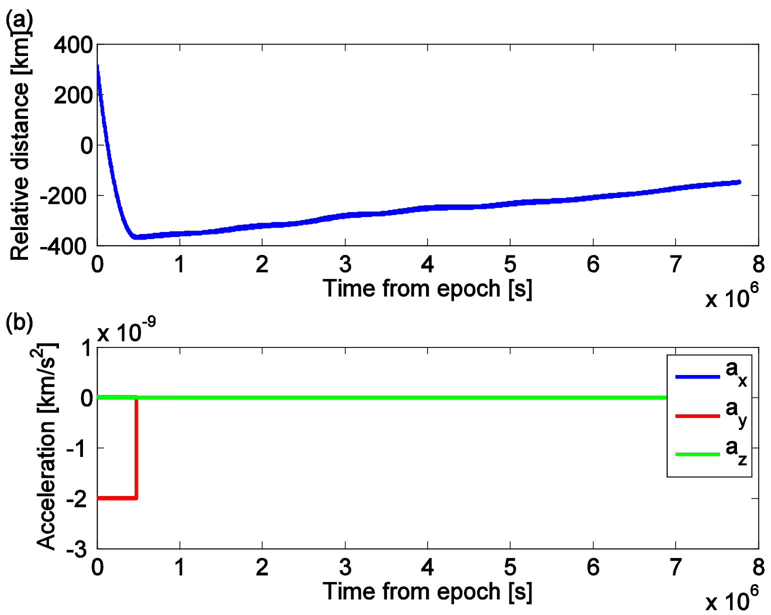

Figure 2. Phasing maneuver using a non-linear simulation: (a) relative distance (b) applied acceleration, Δa = 2000 m

The phasing maneuver, although efficient, requires accurate knowledge of the orbital parameters of all the spacecraft in the formation. For a pico-satellite with limited sensor capability this is not currently possible, instead, off-line TLE data set is used. As was discussed in section 2 the TLE accuracy and update are insufficient for a phasing controller, with SMA errors as large as 1500 m and update time of 1 – 2 days.

3.2 Simple Orbit Control Law – HCW Model

Immediately after deployment the pico-satellites are in a tight formation. This proximity, the fact that the satellites are launched to a circular orbit, and the negligible differential J2 effect allow the use of the well-known linearized Hill-Clohessy-Wiltshire (HCW) equations [6] for analyzing the effect of continues thrust on the relative spacecraft dynamics. In-track thrusting is again selected as the control strategy as the in-plane HCW equations are fully controllable by the in-track acceleration alone.

In order to find an appropriate solution (or thrust) for controlling the formation an optimal control approach is preferred. An optimal control will minimize the propellant expenditure - keeping the mass flow rate as low as possible while maintaining formation constraints. This criterion can be formed into a quadratic cost for the control (acceleration). As the HCW equations are linear, the cost quadratic, and the target is to bring the deputy near the chief, it is only natural to use the well-known linear quadratic regulator (LQR) solution. However, this analytic solution does not take into account the control constraints, in our case the limited acceleration that can be provided by the thruster. Thus, a model predictive control (MPC) [7] numeric solver is used instead.

In accordance with the data presented in section 2.1 we tested the best case scenario with the following initial conditions: $\Delta a = 30 \text{ m}, \rho = 10 \text{ km}$. The initial position of the deputy was obtained by simulating the drift between the satellites without control thrust for 12 h. The simulation ran for 200 orbits, a total of 14 days. Since a HCW model was used, only the deputy was allowed to actively change its orbital parameters.

As shown in Fig. 3(a), the deputy spacecraft gradually approaches the chief. We observe that the maximum separation is about 18 km in the first half-day, after which the relative distance decreases. After 4.5 days the distance reduces to about 0.5 km and remains at that level. The acceleration component in the in-track direction is shown in Fig. 3(b). We observe that a bang-bang type control is followed until the relative distance reduces to 1 km. A continues acceleration is provided with the direction alternating at the points of closest approach. A positive thrust command is applied for a positive in-track relative distance and a negative thrust command is applied for a negative relative distance. When the distance reduces below 1 km a LQR control is applied since the control acceleration is no longer constrained.

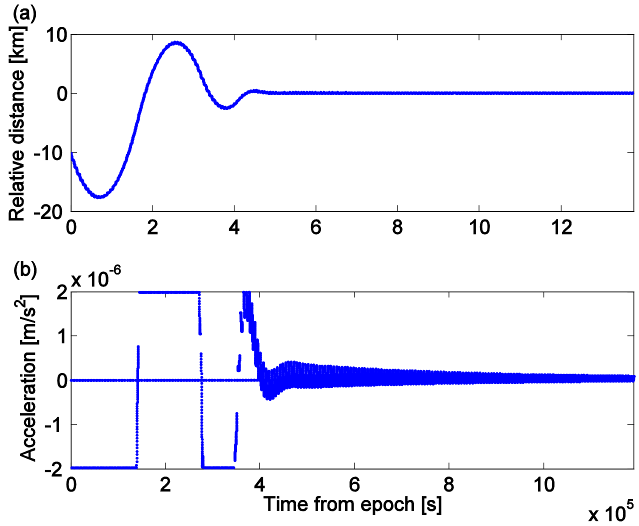

Figure 3. MPC control solution using the HCW model: (a) relative distance (b) applied in-track acceleration, Δa = 30 m

As the time constant of the bang-bang control is measured in days, an on-line orbit determination is not required. A simple ground command using TLE data updates is sufficient and the 1-2 km uncertainty will not change the acceleration control. This type of off-line method allows to greatly simplify the spacecraft's orbit control implementation.

3.3 Simple Orbit Control Law – Non-Linear Simulations

The simple orbit control law was tested using a high precision numerical orbit-propagator, removing the approximations made in the HCW model. Case 3 in Tab. 2 was selected for the initial conditions. A continues acceleration magnitude of 2×10^{-6} m/s^2 was used. The orbits were propagated for 3 months and the results are presented in Fig. 4. We observe that the motion is bounded and the controller is able to keep the deputy at relative distance of less than 1000 km from the chief. In this scenario a total $\Delta V \approx 15$ m/s was used. Similarly, using acceleration of 10^{-6} m/s^2 and $\Delta V \approx 7.5$ m/s, the relative distance was kept below 1500 km (not shown).

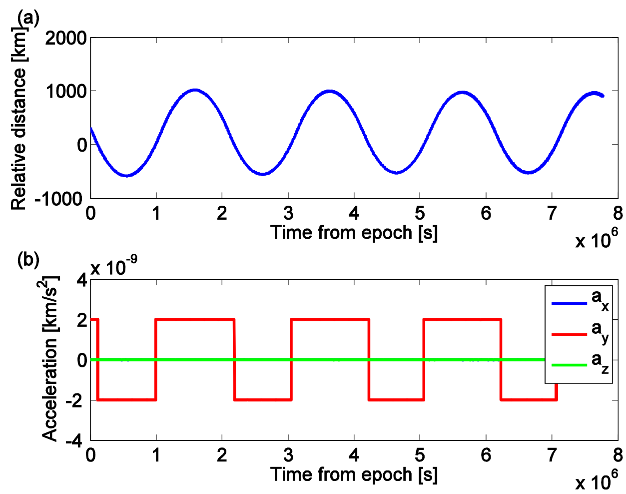

Figure 4. Simple control law using a non-linear simulation: (a) relative distance (b) applied acceleration, Δa = 2000 m

4. Satellite and Propulsion System Design

The UWE-4 is based on a modular CubeSat bus that was developed at Wuerzburg University [8]. The satellite bus includes a comprehensive suite of sensors: sun sensors, magnetometers and rate gyroscopes; six air-coil magnetorquers are mounted one on each exterior panel. In addition to power management, communication, attitude determination and control modules, slots are available for future use.

Volume, mass, and power constraints in pico-satellites require the use of innovative propulsion solutions. Only handful state of the art propulsion systems are currently suitable [9]. Among the few the vacuum arc thruster (VAT), an electric propulsion device, is a promising candidate. This type of thruster is simple, scalable, and has adequate performance in very low power operation [10].

The University of the Federal Armed Forces in Munich (UniBwM) is developing the micro-VAT for the UWE-4 pico-satellite. The propulsion system is composed of two parts: thruster heads and a power processing unit (PPU). UWE-4 utilizes the modular payload slots for accommodating the PPU. The thruster heads are accommodated on the outer structure rails. These rails were originally intended to be used only as interface with the deployment mechanism. In UWE-4, however, the rails are modified to contain the thrusters, thus reducing the propulsion system mass. The satellite layout including the propulsion system is shown in Fig. 5.

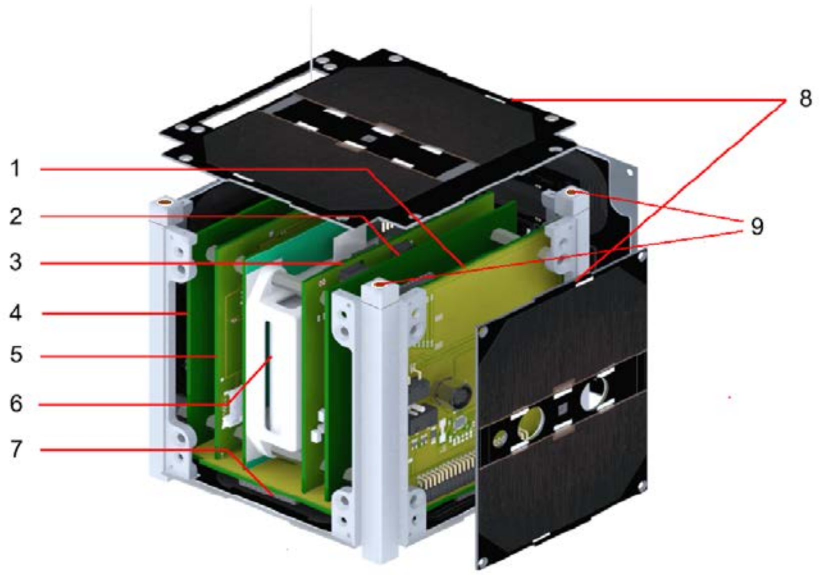

Figure 5. Structural overview of UWE-4: (1) Front Access Board,(2) PPU, (3) ADCS, (4) Communication, (5) OBDH, (6) EPS, (7) Backplane, (8) Panels, and Thruster-Heads (9)

4.1 VAT Operating Principles

The VAT operates when high enough voltage is applied between the anode and cathode to form an arc discharge, as shown in Fig. 6. The discharge is sustained by attaching to the cathode in localized areas, less than 10 µm in diameter, known as cathode spots. Each spot can produce up to hundred amperes by field enhanced thermionic emission [11]. Spot lifetime is < 0.1 µs. Once extinguished another spot is created that leads to an apparent random movement of the cathode spot across the cathode surface.

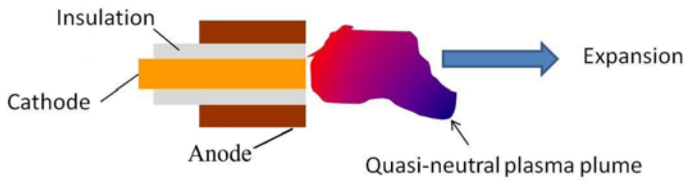

Figure 6. Vacuum arc thruster operation principles

The spot emits electrons and material vapor by explosive emission into the inter-electrode gap. The vapor is fully ionized and the resulting plasma conducts the electron current between cathode and anode. Thrust is created by fast ions that carry about 10 % of the current. The ionized plasma is accelerated by supersonic flow expansion to velocities of ~ 10^4 m/s [10]. The ion flow is mainly directed away from the cathode surface following a cosine distribution [12].

The selection of cathode material is important as it affects the ion current fraction α_i, the ion velocity V_i, and the cathode erosion rate γ_c. The cathode erosion rate is a combination of vapor and macro particles-mass. The neutral macro-particles reduce thruster efficiency as they have low velocities and do not contribute to the thrust. Table 3 summarized the effect of cathode material on these parameters.

Table 3. Ion current and erosion rates, taken for published data [10],[13]

Cathode material	α_i [%]	$\langle V_i \rangle$ [km/s]	γ_c [µg/C]
Sn	11.4	1.37	80.5
Al	11.2	5.93	28
W	5	10.57	55

An important advance has enabled the miniaturization of the VAT - the so called triggerless operation [14]. By coating the inter-electrode dielectric gap with thin conducting film (usually a carbon layer) with finite resistance, relatively low voltages of few hundred volts are required to ignite the discharge. The triggerless thruster was operated successfully for more than 10^5 pulses at low energy (100 mJ).

4.2 Power Processing Unit

As in all electric propulsion devices the thrust generated is depended on thruster efficiency and available power. When not in the umbra, the UWE-4 generates approximately 2.5 W of continues power of which about 2 W is available to the propulsion system. With thrust to power ratio between 1 – 10 µN/W, impulse bit of > 1 µNs is expected.

An efficient power processing unit (PPU) is necessary to condition the continues voltage and current of (~ 4 V and 0.5 A respectively) produced by the photovoltaic cells to the required VAT pulse operation with voltage of 20 - 30 V and current above 10 A.

The PPU for the UWE-4 project is developed and manufactured by Apcon Aerospace and Defense GmbH. The electronics are mounted on a single standard subsystem module. The PPU is comprised of three sections: 1) a DC/DC convertor from bus voltage to 12 V; 2) SEPIC - converts from 12 V to 25 V and includes a large capacitor; 3) a switched inductive front end.

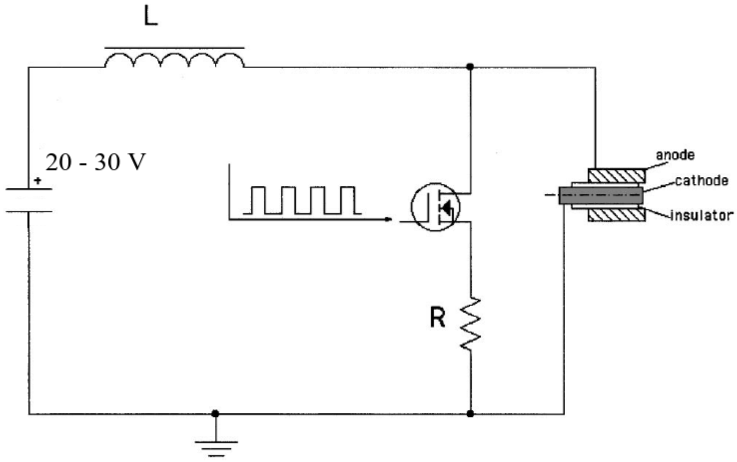

Figure 7. Electrical scheme of the switched inductive front end

The SEPIC buffers the bus power supply from the relatively high current used during the thrust pulse. The switched inductive front end is charged from the capacitor and releases its energy through the VAT by opening the transistor switch (SCR) shown in Fig. 7. When the switch is opened voltage peak of $L\,dI/dt$ is created that breaks down the thin coating between anode and cathode. A typical measurement of the discharge current and voltage during a single pulse is provided in Fig. 8.

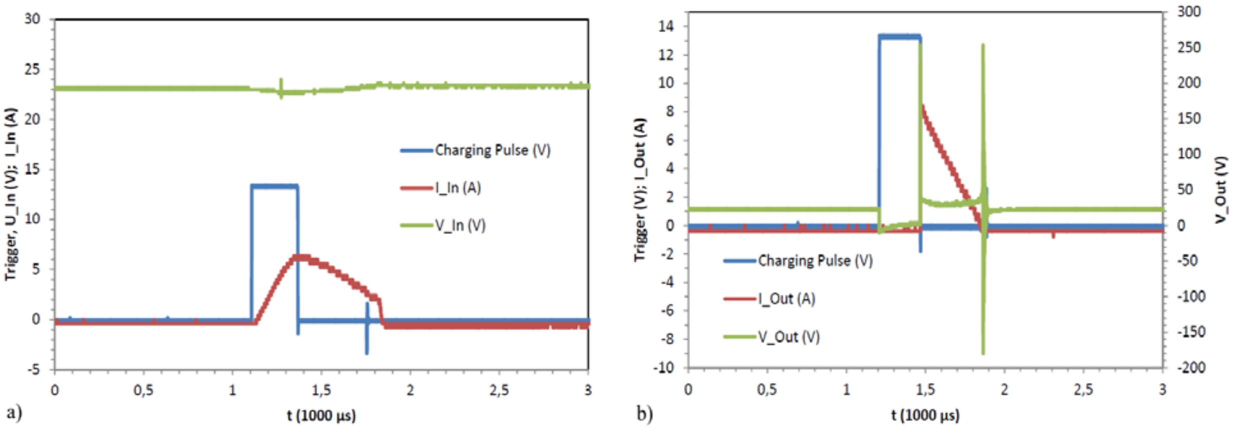

Figure 8. Electrical measurements of the switched inductive front end. Input (a) and output (b) at 24 V using copper cathode

The PPU is designed to generate pulse energies between 10 – 1000 mJ with a pulse frequency of 1 - 10 Hz. The pulse energy and frequency is digitally controlled. The

PPU also provides for fault protection and is tasked with sampling the discharge current and voltage. During the mission it is planned that the PPU data will be stored on the S/C OBDH and then transmitted to the ground station for analysis.

5. Conclusions

The feasibility of maintaining a tight formation of pico-satellites using very-low-thrust electric propulsion was investigated. By following mission requirement and system performance, a simple off-line control method was developed. This scheme requires only TLE data with daily ground command. High precision simulations show that in order to maintain a bounded formation of 1500 km an average ΔV of 2.5 m/s per month is required. The simplicity of the control law provides important advantage for application in a pico-satellite with extremely limited resources. The implementation of the vacuum arc thruster propulsion system on board the UWE- 4 pico-satellite is presented. Further research is being conducted to improve life time and performance of the thruster including: optimal operation regime, thruster head design, and cathode material.

6. Acknowledgements

Support for this research was provided by the Bavarian Space Technology Program from the project "Innovative propulsion system for satellite formations based on vacuum arc thrusters". I.K. acknowledges the Minerva Foundation for the financial support.

7. References

[1] Richards, M.G., Viscito, L., Ross A.M., and Hastings D.E.,"Distinguishing Attributes for the Operationally Responsive Space Paradigm", In Proceedings of 6th Responsive Space Conference, 2008, AIAA-RS6-2008-1004.

[2] Remuss., N. L., "Responsive Space for Europe", In ESPI Report, Vol. 22, 2010, ESPI European Space Policy Institute.

[3] Alfriend, K.T., Vadali, S.R., Gurfil, P., How, J.P., and Breger, L.S., *Spacecraft Formation Flying: Dynamics, Control and Navigation*, 2010, Elsevier Astrodynamics.

[4] Schilling, K., and Schmidt., M., "Communication in Distributed Satellite Systems", in book *Distributed Space Missions for Earth System Monitoring* edited by D'Errico, M., 2010, pp. 345 – 354, Springer, New York.

[5] Cubesat Design Specification, rev.12, 2009, Stanford University and California Polytechnic Institute.

[6] Clohessy, W. H., and Wiltshire, R. S., "Terminal Guidance for Satellite Rendezvous," Journal of Aerospace Sciences, Vol. 27, 1960, pp. 653-658.

[7] Maciejowski, J., *Predictive Control with Constraints*, 2002, Pearson Education, England.

[8] Busch, S., and Schilling, K., “UWE-3: A Modular System Design for the Next Generation of Very Small Satellites”, In Proceedings of Small Satellites Systems and Services - The 4S Symposium 2012, 2012.

[9] Mueller, J., Hofer, R., Ziemer, J., “Survey of Propulsion Technologies Applicable to Cubesats“, http://hdl.handle.net/2014/41627, last accessed April 2013.

[10] Polk, J.E., Sekerak, M.J., Ziemer, J.K., Schein J., Qi, N., and Anders, A., “Theoretical Analysis of Vacuum Arc Thruster and Vacuum Arc Ion Thruster Performance”, IEEE Trans. on Plasma Sci., Vol. 36, No. 5, 2008, pp. 2167-79.

[11] Jüttner, B., "Cathode Spots of Electric Arcs", J. Phys. D: Appl. Phys., Vol. 34, 2001, pp. 103–123.

[12] Kutzner, J., and Miller H.C., “Ion Flux From the Cathode Region of a Vacuum Arc”, IEEE Trans. on Plasma Sci., Vol. 17., No. 5., 1989, pp. 713-16.

[13] Anders, A., Oks, E.M., Yushkov, G.Y., Savkin, K.P., Brown I.G., and Nikolaev, A.G., “Measurements of the Total Ion Flux From Vacuum Arc Cathode Spots”, IEEE Trans. on Plasma Sci., Vol. 33, No. 5, 2005, pp. 1532-36.

[14] Schein et al., “Inductive Energy Storage Driven Vacuum Arc Thruster”, Review of Scientific Instruments, Vol. 73, No. 2, 2002, p. 925-7.